EFFECT OF MOUNT ANGLE ON STATIC AND DYNAMIC CHARACTERISTICS OF GAS-LUBRICATED, NONCIRCULAR JOURNAL BEARINGS[*]

A. D. RAHMATABADI[**] AND R. RASHIDI

Dept. of Mechanical Engineering, Yazd University, Yazd, I. R. of Iran
Email: dashti@yazduni.ac.ir

Abstract– In the case of noncircular journal bearings, as opposed to circular journal bearings, the orientation of bearing with respect to a given load direction can be a design parameter. This orientation may be defined in terms of an angle, which in the present work is being referred to as the mount angle. The purpose of the work presented in this paper is to study the effect of the mount angle on the theoretical static and dynamic characteristics of three types of gas-lubricated noncircular bearings. It is found that the effect of the mount angle happens to be more pronounced at low compressibility numbers. Also, among the three types of bearings, the effect of the mount angle is more significant in two lobe bearings in comparison to the three and four lobe bearings.

Keywords– Gas-lubrication, noncircular bearing, mount angle, stability characteristics

1. INTRODUCTION

The term bearing mounting refers to the orientation of a bearing with respect to a fixed load direction and is typical to the lobed and pad-type bearings. The bearing mounting may be expressed in terms of an angle, to be referred to as the mount angle θ_M, by which a bearing is set by turning with respect to a vertical load support; (see Fig. 1 in which the mount angle is defined for three types of lobed bearings). As shown, the mount angle is taken positive when a bearing is turned in the direction of rotation. For usual upright configurations, $\theta_M = 0$.

In the bearing literature, the bearing analysis and characteristics are invariably reported for upright configurations; (see the work of Chandra *et al*. [1] on gas-lubricated lobed bearings and the references cited therein). In the present work, the effect of the mount angle on the static and dynamic performance characteristics of the three types of gas-lubricated lobed bearings is studied. The lobed bearings considered are two, three, and four lobe bearings of symmetric geometries as shown in Fig. 1. It is believed that studies of this kind are not available in the literature, and, therefore, fill a void in the existing bearing literature.

The analysis describing the governing equations, their solution, and results are given in the succeeding sections. The Galerkin finite element method [2] is used for the computational formulation of the governing equations. The governing Reynolds equation of gas lubrication for static analysis is nonlinear and its solution scheme is based on Newton's method; this is adopted from the work of Rohde and Oh [3]. The dynamic analysis is based on Lund's work [4, 5].
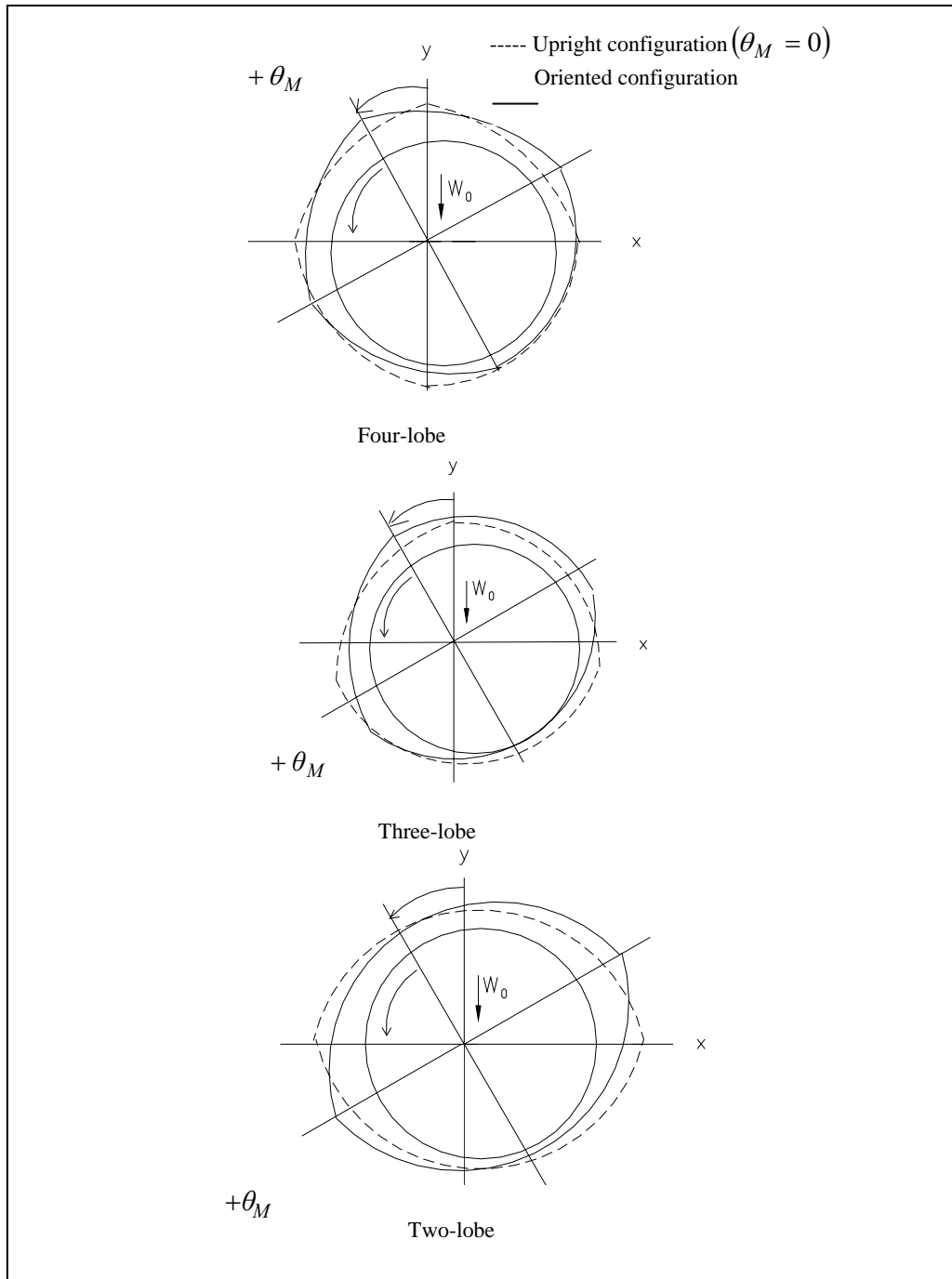

[**]Corresponding author

Fig. 1. Upright and oriented configurations

2. ANALYSIS

The geometric details of a representative noncircular bearing configuration are shown in Fig. 2.

Analysis of a gas-lubricated noncircular bearing involves the solution of the governing equations separately for an individual lobe of the bearing, treating each lobe as an independent partial bearing. To generalize the analysis for all noncircular geometries, the film geometry of each lobe is described with reference to bearing fixed Cartesian axes (Fig. 2). Thus the film thickness in the clearance space of the kth lobe, with the journal in a state of translatory whirl, is expressed as [1]

$$h_k = \frac{1}{\delta} - X_j \cos\theta - Y_j \sin\theta + (\frac{1}{\delta} - 1)\cos(\theta - \theta_0^k) \tag{1}$$

and

$$h_{ok} = \frac{1}{\delta} - X_{j0} \cos\theta - Y_{j0} \sin\theta + (\frac{1}{\delta} - 1)\cos(\theta - \theta_0^k) \tag{2}$$

is the steady state film thickness. (X_{j0}, Y_{j0}) and (X_j, Y_j) are respectively the steady state and dynamic journal center coordinates and δ is the preload in the bearing. Also θ_0^k is the angle of lobe line of centers. The pressure governing equation of the isothermal flow field in a bearing lobe is [6]

$$\frac{\partial}{\partial\theta}\left\{h^3(P+1)\frac{\partial P}{\partial\theta}\right\} + \frac{\partial}{\partial\xi}\left\{h^3(P+1)\frac{\partial P}{\partial\xi}\right\} = \Lambda\left[U\frac{\partial}{\partial\theta} + 2\frac{\partial}{\partial t}\right]\{(P+1)h\} \tag{3}$$

subjected to the conditions

$$P(\theta_1^k, \xi, t) = P(\theta_2^k, \xi, t) = P(\theta, \pm\lambda, t) = 0 \tag{4}$$

where θ_1^k and θ_2^k are, respectively, the leading and trailing edge boundaries of the kth lobe.

To describe the dynamic state of the flow field, the whirling motion of the journal is assumed to be harmonic [1, 2], that is

$$X' = \text{Re}(|X'|e^{j\hbar t}), \quad Y' = \text{Re}(|Y'|e^{j\hbar t}) \tag{5}$$

where X', Y' are the perturbation coordinates of the journal measured from its static equilibrium position, $|X'|, |Y'|$ are the motion amplitudes, and $j = \sqrt{-1}$.
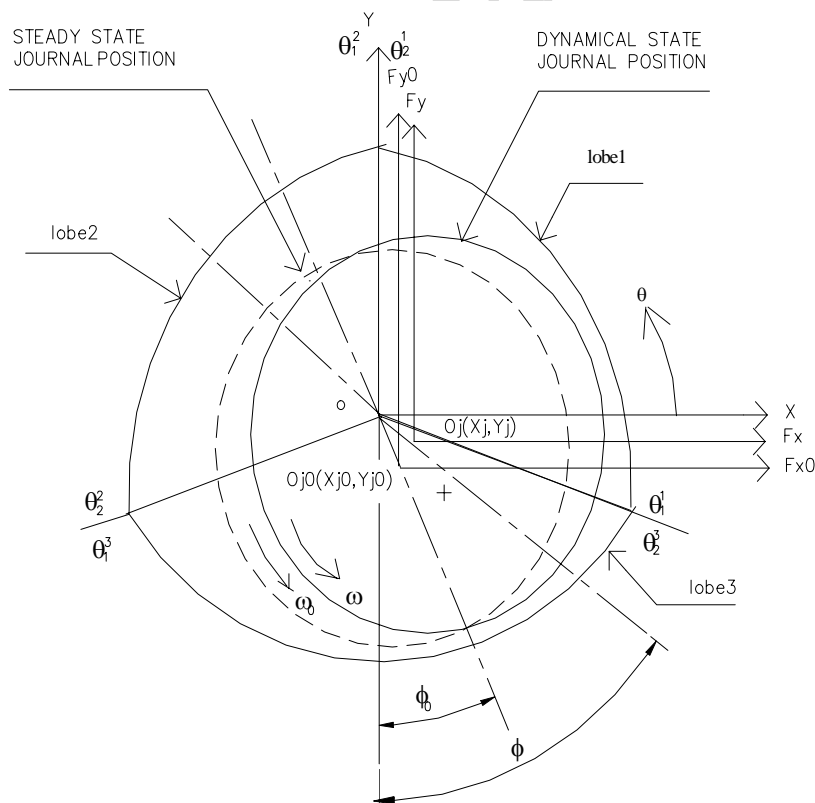

Fig. 2. Noncircular (three lobe) bearing geometry and coordinate axes

The gas pressure may be expressed as the sum of the steady state pressure (P_0) and the dynamic pressure. To a first approximation

$$P = P_O + P'_x \ X' + P'_y Y' \tag{6}$$

where

$$P'_x = P_x + j\gamma P_{\dot{x}}, P'_y = P_y + j\gamma P_{\dot{y}} \tag{7}$$

are the dynamic pressure components. The steady state pressure equation, obtained by substituting Eq. (6) in Eq. (3) and putting $X' = Y' = 0$, is

$$\frac{\partial}{\partial \theta}\left\{ h_0{}^3 (P_0 + 1)\frac{\partial P_0}{\partial \theta}\right\} + \frac{\partial}{\partial \xi}\left\{ h_0{}^3 (P_0 + 1)\frac{\partial P_0}{\partial \xi}\right\} = \Lambda \frac{\partial}{\partial \theta}\big[(P_0 + 1)h_0\big] \tag{8}$$

The equations for P'_x and P'_y are obtained by partial differentiation of Eq. (3) with respect to X' and Y'

$$\frac{\partial}{\partial \theta}\left\{ h_0{}^3 (P_0 + 1)\frac{\partial P'_Z}{\partial \theta} + h_0{}^3\frac{\partial P_0}{\partial \theta} P'_Z - \Lambda h_0 P'_Z\right\} + \frac{\partial}{\partial \xi}\left\{ h_0{}^3 (P_0 + 1)\frac{\partial P'_Z}{\partial \xi} + h_0{}^3\frac{\partial P_0}{\partial \xi} P'_Z\right\}$$

$$- j2\gamma\Lambda h_0 P'_Z = \frac{\partial}{\partial \theta}\left\{ f(\theta)(P_0 + 1)(3h_0{}^2\frac{\partial P_0}{\partial \theta} - \Lambda)\right\} + \frac{\partial}{\partial \xi}\left\{ 3h_0{}^2 f(\theta)(P_0 + 1)\frac{\partial P_0}{\partial \xi}\right\} \tag{9}$$

$$- j2\gamma\Lambda(P_0 + 1)f(\theta)$$

where P'_z stands for P'_x or P'_y, that is

$$P'_z = P_z + j\gamma P_{\dot{z}} \quad, z = x, y \tag{10}$$

and

$$f(\theta) = \begin{cases} \cos\theta & \text{for} \ P'_x \\ \sin\theta & \text{for} \ P'_y \end{cases} \tag{11}$$

In the present work, the Galerkin finite element method [2] is used for the computational formulation of the governing equations, Eqs. (8) and (9). The governing equation for steady state pressure, Eq. (8), is nonlinear. The scheme for its solution is based on the Newton's method; the details of the same may be found in [1] and [3]. The governing equations for dynamic pressure components, Eq. (9), are complex; however, the finite element formulation poses no difficulty as Eq. (9) is linear.

3. STATIC CHARACTERISTICS

Having obtained the steady state pressure field by the solution of Eq. (8),the static characteristics are obtained. The static characteristics are described by the bearing load capacity, the attitude angle and the viscous power loss. The components of the gas film force on the journal are given by

$$\begin{bmatrix} F_{x0} \\ F_{y0} \end{bmatrix} = \sum_{k=1}^{L}\begin{bmatrix} F_{x0}^k \\ F_{y0}^k \end{bmatrix} = -\sum_{k=1}^{L}\int_{-\lambda}^{\lambda}\int_{\theta_1^k}^{\theta_2^k} P_{0k}\begin{bmatrix} \cos\theta \\ \sin\theta \end{bmatrix} d\theta d\xi \tag{12}$$

where L stands for the number of lobes.

The load capacity and the attitude angle are then given by

$$F_0 = (F_{x0}^2 + F_{y0}^2)^{1/2} \ , \ \phi_0 = \arctan(X_{j0} / Y_{j0}) \tag{13}$$

The viscous power loss is given by

$$P_L = \sum_{K=1}^{L}\int_{-\lambda}^{\lambda}\int_{\theta_1^k}^{\theta_2^k}(\frac{3h_{0k}}{\Lambda}\frac{\partial P_{0k}}{\partial \theta} + \frac{1}{h_{0k}})d\theta d\xi \tag{14}$$

4. DYNAMIC CHARACTERISTICS

The components of resultant gas film force on the journal may be expressed as

$$\begin{Bmatrix} F_x \\ F_y \end{Bmatrix} = \begin{Bmatrix} F_{x0} \\ F_{y0} \end{Bmatrix} - \begin{bmatrix} Z_{xx} & Z_{xy} \\ Z_{yx} & Z_{yy} \end{bmatrix} \begin{Bmatrix} \dot{X}' \\ \dot{Y}' \end{Bmatrix} = -\sum_{k=1}^{L} \int_{-\lambda}^{\lambda} \int_{\theta_1^k}^{\theta_2^k} P_i \begin{Bmatrix} \cos\theta \\ \sin\theta \end{Bmatrix} d\theta d\xi \tag{15}$$

that

$$Z_{mn} = S_{mn} + j\gamma B_{mn} \qquad\qquad (m, n = x, y) \tag{16}$$

It now follows from Eqs. (6) and (15) that

$$\begin{bmatrix} Z_{xx} & Z_{xy} \\ Z_{yx} & Z_{yy} \end{bmatrix}^T = \sum_{k=1}^{L} \int_{-\lambda}^{\lambda} \int_{\theta_1^k}^{\theta_2^k} \begin{bmatrix} P_x' \\ P_y' \end{bmatrix} [\cos\theta \quad \sin\theta] d\theta d\xi \tag{17}$$

It is clear from Eqs. (7), (16) and (17) that the coefficients S_{mn} correspond to the film force reaction components of reals of P_x' and P_y', i.e P_x and P_y. Similarly the coefficients B_{mn} correspond to the film force components of the imaginary parts of P_x' and P_y', i.e $\gamma P_{\dot{x}}$ and $\gamma P_{\dot{y}}$. It should also be noted from Eq. (8) that P_x' and P_y', and hence the gas film dynamic coefficients, depend on the whirl frequency ratio γ.

5. STABILITY MARGIN

The stability of the motion of journal in free translatory whirl is

$$M \begin{bmatrix} \ddot{X}' \\ \ddot{Y}' \end{bmatrix} + \begin{bmatrix} B_{xx} & B_{xy} \\ B_{yx} & B_{yy} \end{bmatrix} \begin{bmatrix} \dot{X}' \\ \dot{Y}' \end{bmatrix} + \begin{bmatrix} S_{xx} & S_{xy} \\ S_{yx} & S_{yy} \end{bmatrix} \begin{bmatrix} X' \\ Y' \end{bmatrix} = \begin{bmatrix} 0 \\ 0 \end{bmatrix} \tag{18}$$

Where M is the journal mass.

Substituting Eq. (5) in Eqs. (18) it can easily be shown that the characteristics equation of the translatory limit cycle is

$$(-M\gamma^2 + S_{xx} + j\gamma B_{xx})(-M\gamma^2 + S_{yy} + j\gamma B_{yy}) - (S_{xy} + j\gamma B_{xy})(S_{yx} + j\gamma B_{yx}) = 0 \tag{19}$$

Which on separating the real and imaginary parts gives

$$M\gamma^2 = (S_{xx}B_{yy} + S_{yy}B_{xx} - S_{xy}B_{yx} - S_{yx}S_{xy})/(B_{xx} + B_{yy}) \tag{20}$$

$$\gamma^2 = \left[(S_{xx} - M\gamma^2)(S_{yy} - M\gamma^2) - S_{xy}S_{yx}\right]/(B_{xx}B_{yy} - B_{xy}B_{yx}) \tag{21}$$

The above equations provide the criterions for the determination of γ and the stability margins. Quite obviously there would be a unique combination of the frequency ratio and the dynamic coefficients which satisfy, simultaneously, Eqs. (9) and (21).

Corresponding to the value of the frequency ratio of the film induced whirling, the stability margin may be expressed from Eq. (22) as:

$$M_c = (S_{xx}B_{yy} + S_{yy}B_{xx} - S_{xy}B_{yx} - S_{yx}B_{xy})/\left[(B_{xx} + B_{yy})\gamma^2\right] \tag{22}$$

Where M_c may be referred to as the critical mass parameter of the journal bearing system.

The dynamic coefficients, critical mass parameter and the whirl frequency ratio at the threshold of instability are determined by trials [4, 5].

6. RESULT AND DISCUSSION

In this paper the effect of the mounting angle on the three bearing forms, namely, two lobe, three lobe and four lobe bearings is investigated. The preload for each bearing is taken as 0.5 and the nondimensional external load is taken as $W_0 = 1$. Also, the bearing aspect ratio has throughout been taken as unity, which is the most commonly used value in practical applications. The range of mount angle for each bearing is taken as one half of lobe arc length on both sides of the load vector. Thus the ranges of the mount angles are: $\pm 90^0$ for two lobe bearing, $\pm 60^0$ for three lobe bearing and $\pm 45^0$ for four lobe bearing. The computed results are plotted in Figs. 3 to 6.
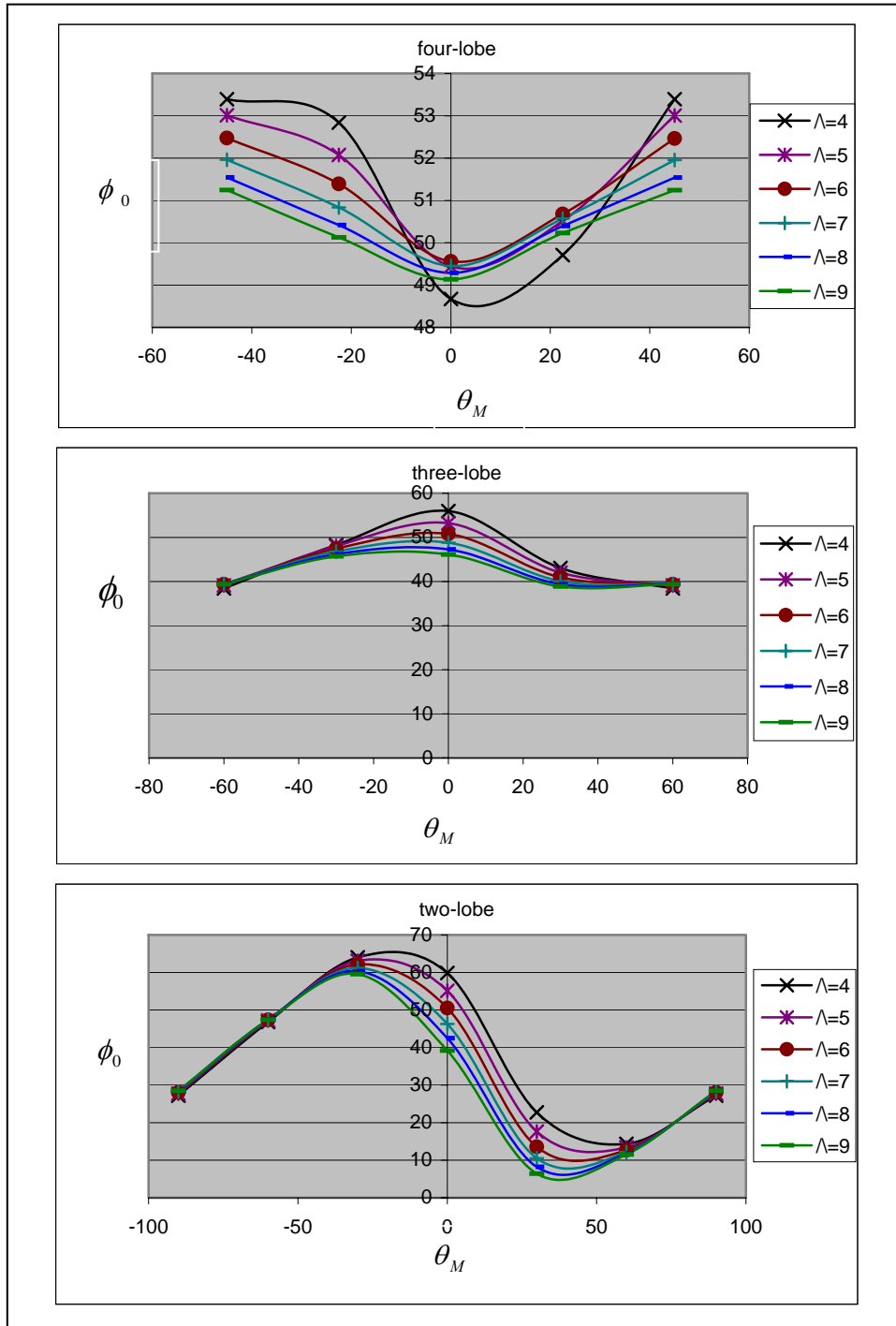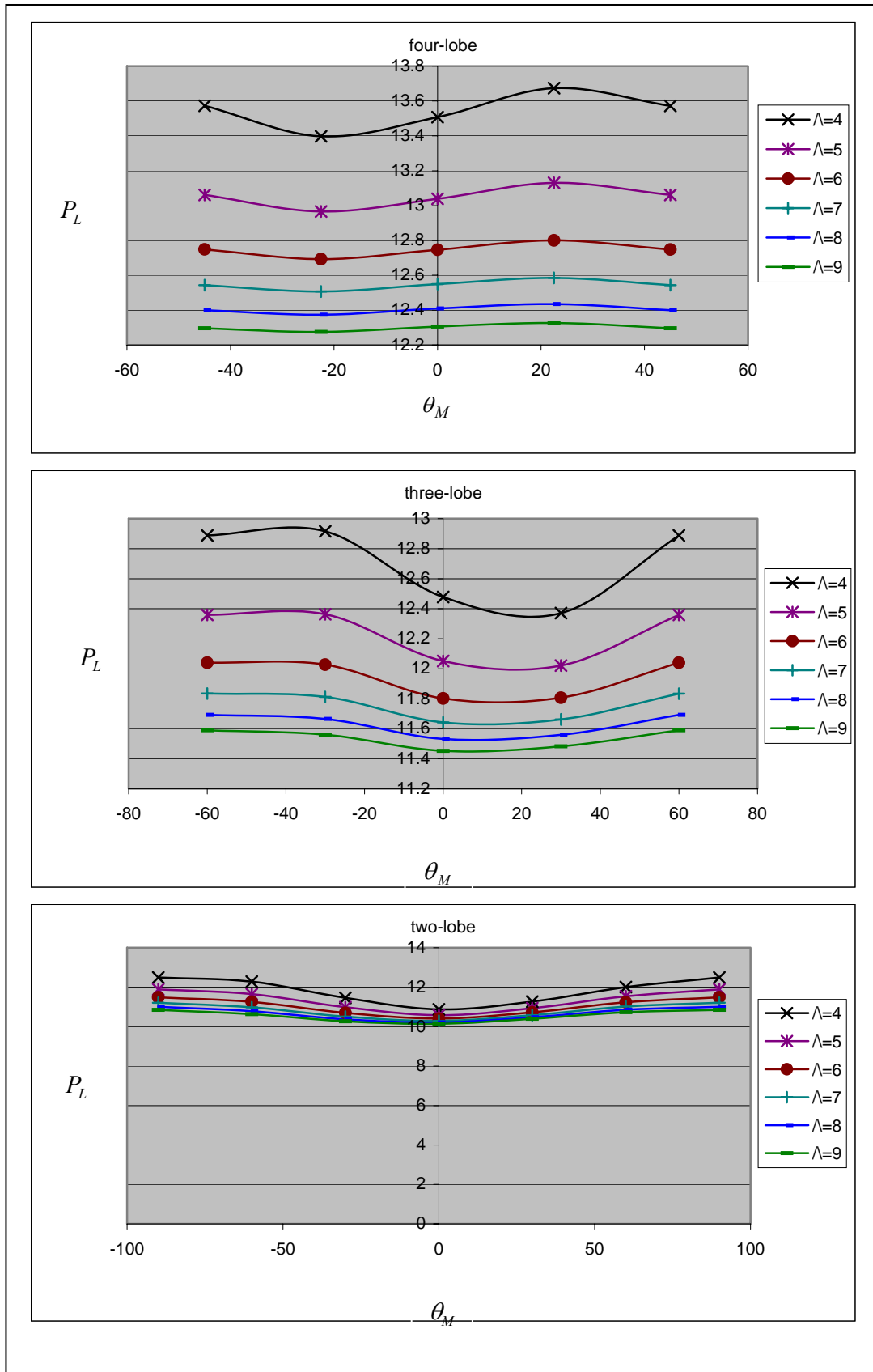

Fig. 3. Effect of mount angle on attitude angle

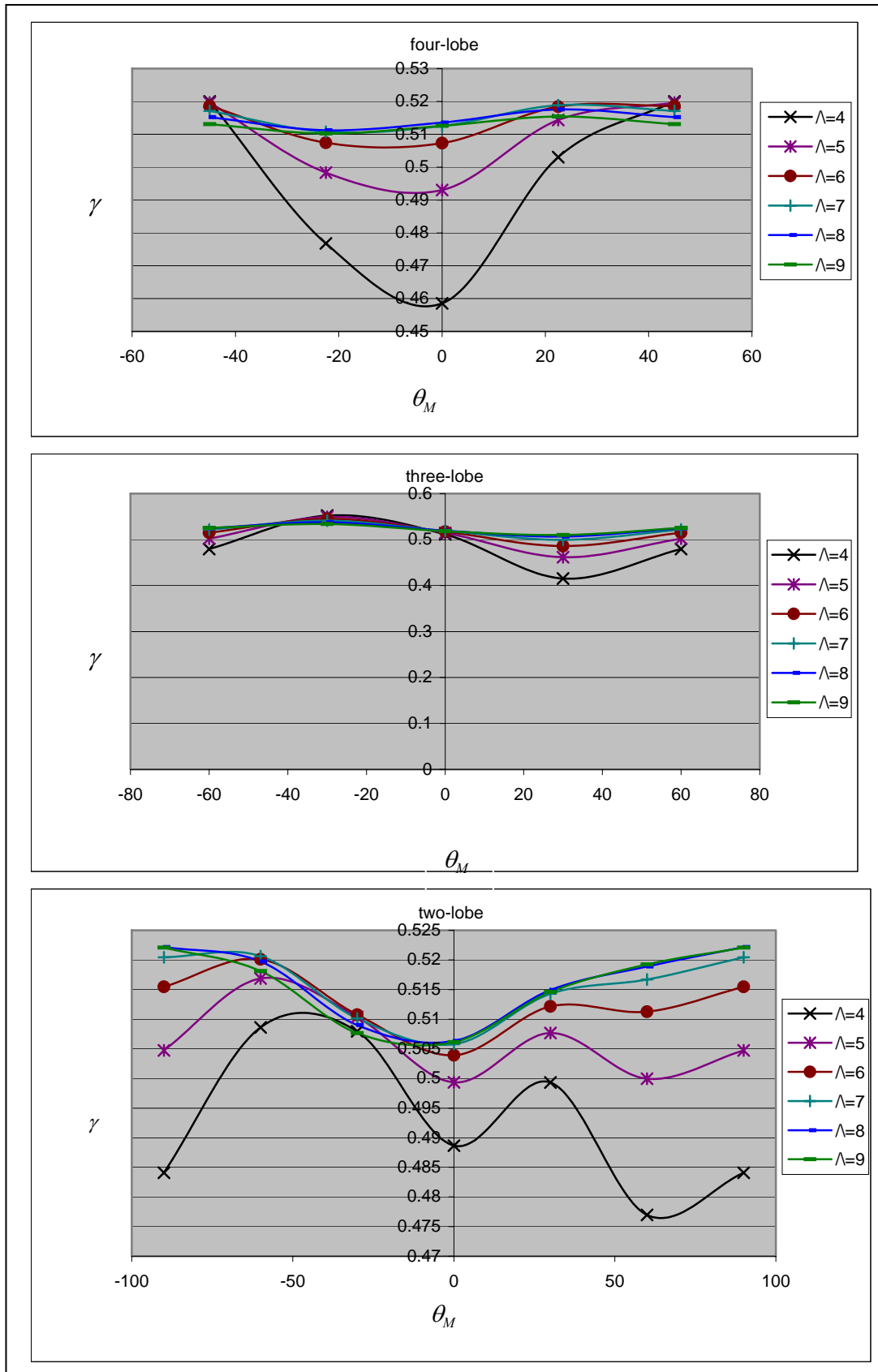Fig. 4. Effect of mount angle on power loss

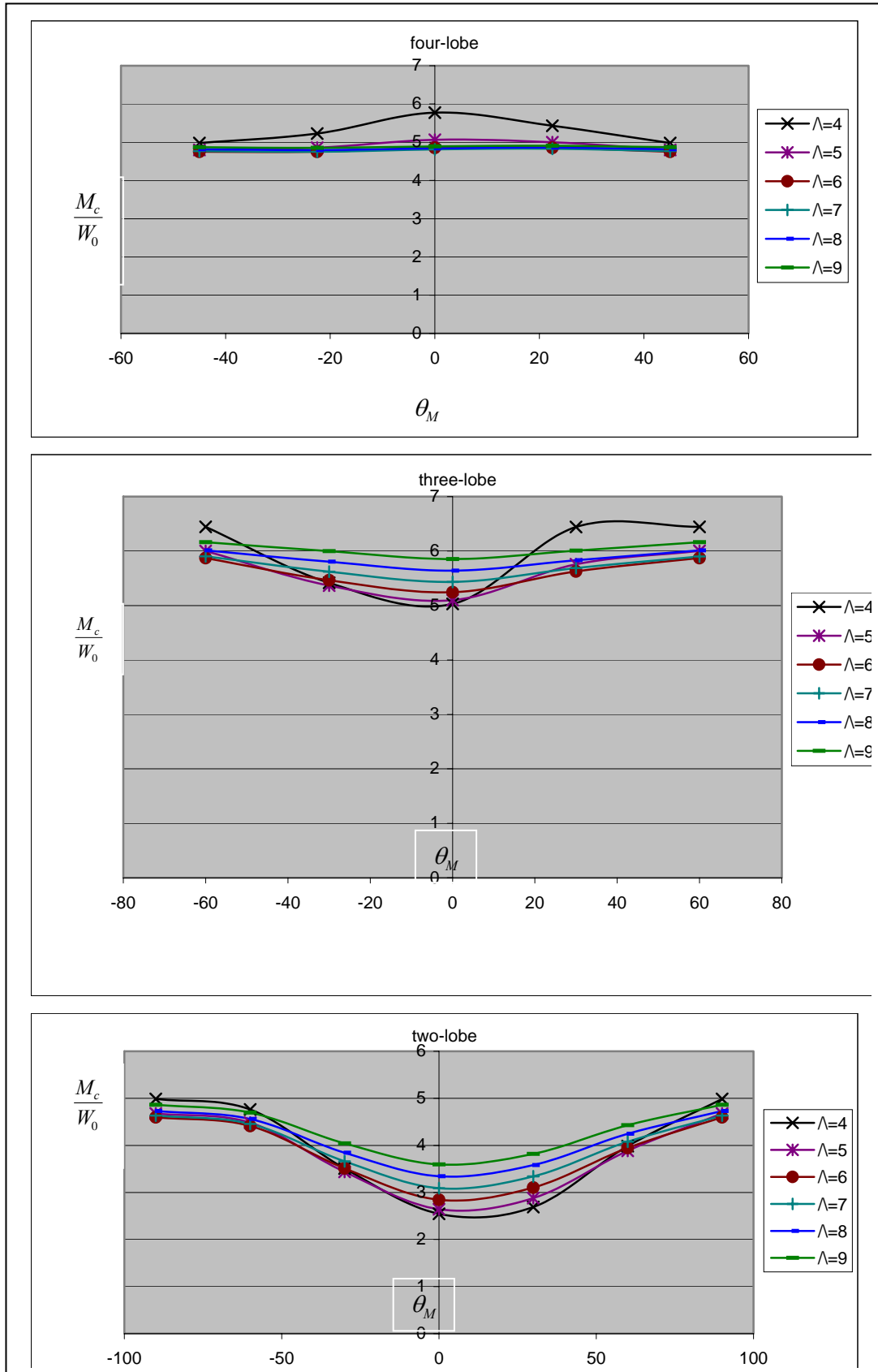Fig. 5. Effect of mount angle on whirl frequency ratio, γ

Fig. 6. Effect of mount angle on critical mass, M_c

The results are:

1. Except for the two lobe bearings, the effect of the bearing mount on the performance characteristics of the three and four lobe bearings is marginal. This is apparently for the reason that three and four lobe geometries are close to the plane axial groove journal bearing and the relative change of geometry due to the rotation of the bearing with respect to a fixed load direction is less compared to that in two lobe bearings.

2. Figure 3 shows that for three and four lobe bearing, changes of attitude angle with mount angle are not significant. However, the two lobe bearing shows a marked variation in the attitude angle with mount angle.

3. From Fig. 4 it is clear that for two lobe bearing the minimum power loss will be at $\theta_M = 0$ and any change in θ_M will increase the power loss. In the case of three and four lobe bearings the effect of the mount angle at a high compressibility number is negligible, while for a low compressibility number there will be changes in power loss.

4. The effect of the mount angle on whirl frequency ratio is shown in Fig. 5 and its effect on the stability parameter is illustrated in Fig. 6. Three and four lobe bearings do not show any change in the stability parameter with the mount angle. However, mount angle has a very significant effect on the dynamic stability of a two lobe journal bearing system. From Fig. 6, it is seen that the mount angle can improve the stability margin by as much as 70%.

7. CLOSURE

In contrast to the plain circular bearing, noncircular and pad-type journal bearing may be oriented in various ways with respect to a given direction of external load. This orientation may be described in terms of an angle, which in the present work has been referred to as the mount angle. In this work, based on the finite element solutions of gas lubrication equations, the effect of the mount angle is studied for three types of gas-lubricated noncircular bearings. Both static and dynamic characteristics of the bearings are considered. It is found that the effect of the mount angle is generally marginal. However, the mount angle is a design parameter and may be selected to meet some specific design goals. Of the three types of bearings considered, the two lobe bearings are most sensitive to the mount angle. Also, the effect of the mount angle decreases with an increase in the compressibility number.

NOMENCLATURE

$\overline{B}_{mn}$	$B_{mn}\overline{P}_a\overline{R}^2/(\overline{C}_m\overline{\omega})$, gas film damping coefficients(Ns/m); m, n = x, y
$\overline{C}$	conventional radial clearance (m), Fig. 2
$\overline{C}_m$	minor clearance when journal and bearing geometric centers are coincident(m)
$\overline{F}$	$F\overline{P}_a\overline{R}^2$, film force on the journal (N)
$\overline{h}$	$h\overline{C}_m$, film thickness (m)
$\overline{M}_c$	$M_c\overline{P}_a\overline{R}^2/(\overline{C}_m\overline{\omega})$, critical mass parameter (Kg)
$\overline{P}$	$P\overline{P}_a$, subambient gas pressure (N/m^2)
$\overline{P}_a$	ambient pressure (N/m^2)
$\overline{P}_L$	$P_L\overline{\mu}\overline{R}^4\overline{\omega}^2/\overline{C}_m$, frictional power loss (Watt)
$\overline{R}$	journal radius (m)
$\overline{S}_{mn}$	$S_{mn}\overline{P}_a\overline{R}^2/\overline{C}_m$, gas film stiffness coefficients (N/m); m, n = x, y

$\bar{t}$	$t/\bar{\omega}_0$, Time (s)
$\overline{U}\ U/\left(\overline{R}\overline{\omega}_0\right)$	instantaneous peripheral speed of the journal (m/s)
$\overline{W}\ W\left(\overline{P_a}\overline{R}^2\right)$	bearing load capacity (N)
x, y	Cartesian axes with origin at bearing geometric center, Fig. 2, subscript for components
x_j, y_j	coordinates of journal center in dynamical state, Fig. 2
x_{j0}, y_{j0}	coordinates of journal center in steady state, Fig. 2
δ	$\overline{C}_m/\overline{C}$ preload in the bearing
ϕ	attitude angle
γ	whirl frequency ratio at the threshold of instability
$\overline{\mu}$	ambient dynamic viscosity of the lubricant (Ns/m^2)
θ	angular coordinate measured from x-axis, Fig. 2
θ_0^k	angle of lobe line of centers
θ_1^k, θ_2^k	angles at the leading and trailing edge of the lobe, Fig. 2
θ_M	Mount angle, Fig. 1
$\overline{\omega}$	rotational speed of the journal (1/s)
ξ	$\overline{\xi}/\overline{R}$, coordinate along bearing axis measured from midspan
λ	bearing lenght to diameter ratio, aspect ratio
Λ	$6\overline{\mu}\overline{\omega}\mathrm{R}/\left(\overline{P}_a\overline{C}_m^2\right)$, compressibility number
k	subscript and superscript for lobe designation
0	subscript for steady state

REFERENCES

1. Chandra, M., Malik, M. & Sinhasan, R. (1983). Comparative study of four gas-lubricated noncircular journal bearing configurations. *Tribology International, 16*(2), 103-108.
2. Reddy, J. (1984). *An introduction to the finite element method*. McGraw-Hill, U.S.A.
3. Rohde, S. M. & Oh, K. P. (1975). Higher order finite element methods for the solution of compressible porous bearing problems. *Int. Journal for Numerical Methods in Eng., 9*, 903-911.
4. Lund, J. W. (1967). A theoretical analysis of whirl instability and pneumatic hammer for a rigid rotor in pressurized gas journal bearings. *J. Lubr. Tech., Trans ASME, 89*, 154-166.
5. Lund, J. W. (1968). Calculation of stiffness and damping properties of gas bearing. *J. Lubr. Tech., Trans. ASME, 90*, 793-803.
6. Frene, J., Nicolas, D., Degueurce, B., Berthe, D. & Godet, M. (1997). Hydrodynamic lubrication-bearing and thrust Bearing. Elsevier Science, The Netherlands.